Thiol-Capped Gold Nanoparticles on Graphite: Spontaneous Adsorption and Electrochemically Induced Release

D. Grumelli, C. Vericat, G. Benitez, M. E. Vela, and R. C. Salvarezza*

Instituto de Investigaciones Fisicoquímicas Teóricas y Aplicadas (INIFTA) Facultad de Ciencias Exactas, Universidad Nacional de La Plata−CONICET, Sucursal 4 Casilla de Correo 16, (1900) La Plata, Argentina

L. J. Giovanetti, J. M. Ramallo-López, and F. G. Requejo

Instituto de Investigaciones Fisicoquímicas Teóricas y Aplicadas (INIFTA) and Instituto de Física La Plata (IFLP) Facultad de Ciencias Exactas, Universidad Nacional de La Plata−CONICET, Sucursal 4 Casilla de Correo 16, (1900) La Plata, Argentina

A. F. Craievich

Institute of Physics, University of Sao Paulo, CEP 05508-900 Sao Paulo, SP, Brazil

Y. S. Shon

Department of Chemistry and Biochemistry, California State University, Long Beach, California 90840

Received: February 16, 2007; In Final Form: February 20, 2007

Gold nanoparticle-(AuNP)-modified carbon graphite surfaces have been prepared by simple immersion of highly oriented pyrolytic graphite (HOPG) in hexane solutions containing 3 nm diameter butanethiol- or nonanethiol-capped nanoparticles. The AuNP adsorb on the HOPG surface free of unbounded thiols, remaining unchanged with time. The amount of adsorbed thiol-protected AuNP depends on concentration and time. The reductive desorption of thiols from the AuNP produces an efficient release of more than 90% of the AuNP from the carbon surface to the aqueous solution. The remaining thiol-free Au nanoparticles do not sinter on the HOPG, forming stable and electrochemically active islands. These results could open interesting possibilities for easy transfer of thiol-capped metallic NP from one environment to another, for controlled release of biomolecules from metallic NP, and for the preparation of catalytic or decontamination systems on large area C surfaces.

Introduction

In the past few years, a great scientific and technological interest has arisen for metallic nanoparticles (NP) supported on different substrates because of their many potential applications in the fields of heterogeneous catalysis,[1] electrocatalysis,[2] biosensors,[3] sensitive analysis, and medical diagnosis.[4] Metallic NP have been used to modify planar surfaces, meso- and nanoporous substrates, nanowires, and carbon nanotubes.[5] In fact, they have been supported on several metals, alloys, zeolites, Si, mica, and C substrates by several methods, including physical vapor deposition,[6] thermal-induced covalent bonding,[7] electrodeposition,[8] and solvent evaporation from solution.[9]

Gold nanoparticles (AuNP) are the most popular nanostructures due to the relatively simple synthesis methods available to obtain highly monodisperse particles of a desired size, both from aqueous and nonaqueous solutions.[10] Thiol-capped AuNP have a wide variety of technological applications, ranging from molecular electronics[11] to medicine.[12]

The attachment of AuNP on carbon surfaces has been a focus of increasing interest. Adhesion of large (15-20 nm) AuNP on glassy carbon modified by electroxidation to yield hydrophilic surfaces has been reported.[13] Also, single- and multiwalled carbon nanotube (CNT) surfaces have been functionalized by different methods[14−18] to allow the covalent attachment of AuNP (either functionalized or not). However, in many cases, covalent attachment of linkers is not desirable because the nanotube electronic properties can be modified,[19] so other AuNP immobilization methods applicable to CNT would be important.

In particular, AuNP on highly oriented pyrolytic graphite (HOPG) can be taken as a model for the AuNP−carbon system and have been prepared by gold electro-[8] and vapor deposition[6] or by solvent evaporation of AuNP chemically prepared in solution.[9] However, electro- and vapor-deposited AuNP yield a broad size distribution,[8] while solvent evaporation, although being a simple strategy to modify C surfaces with high quality thiol-capped AuNP,[20] usually leads to a poor control of the amount of AuNP immobilized on HOPG. Also, in some cases, thiols have been desorbed from the AuNP by thermal treatment at 300 C,[20] although this could result in NP sintering.[21] Thus, other methods to obtain more uniform deposits complemented with efficient cleaning procedures are required.

The spontaneous adsorption of thiol-capped NP from a liquid phase onto nonmodified-carbon substrates could be an attractive strategy that, to our knowledge, has not been systematically explored. In fact, very recently, some evidence has been obtained

* Corresponding author. Fax: 54-221-4254642. Phone: 54-221-4255430. E-mail: robsalva@inifta.unlp.edu.ar.

10.1021/jp071357t CCC: $37.00
Published on Web 04/24/2007

suggesting that this type of NP can be spontaneously adsorbed onto mica surfaces.[22] The results for HOPG could be applied in the future for simple immobilization on CNT, or for large area carbon electrodes, either to build catalytically active surfaces in a simple way, or to remove thiol-capped metal NP from different environments, the latter being an issue of importance for the treatment of nanoparticle residues.

On the other hand, delivery of AuNP carrying biomolecules into living cells has important implications for medical and biochemical purposes, such as controlled release of drugs and disease diagnosis.[23] A controlled and localized release of NP very close to the target is a much desired objective. In particular, carbon is a biocompatible platform to immobilize biomolecule-modified AuNP. Then, by tuning the potential applied to the carbon/aqueous electrolyte interface, a controlled and selective release of the functionalized NP could be possible.

We show here that thiol-capped Au nanoparticles can be adsorbed on nonmodified HOPG by simple immersion in AuNP containing solutions and that the amount of immobilized AuNP depends on their concentration in the solution and adsorption time. Efficient release of nanoparticles takes place during thiol electrodesorption. The remaining thiol-free nanoparticles form isolated nanometer-sized islands on the HOPG that do not change with time. The NP-modified HOPG electrode behaves as a Au electrode without significant modifications even after repetitive voltammetric runs. These results could open interesting possibilities for easy transfer of thiol-capped metallic NP from one environment to another, for controlled release of biomolecules from metallic NP, and for the preparation of catalytic or decontamination systems on large area C surfaces.

Experimental

Gold nanoparticles (AuNP) of 3 nm nominal diameter capped with butanethiol (BT) or nonanethiol (NT) were prepared by the Brust method[24] (see Supporting Information). The real size of these NP dispersed in toluene was determined by small-angle X-ray scattering (SAXS) at the SAXS-1 beamline of the Laboratorio Nacional de Luz Sincrotron (LNLS, Campinas, Brazil). The NP were also characterized in hexane by UV−vis spectroscopy (see Supporting Information). The thiol capped AuNP were immobilized on HOPG by immersing 1 cm^2 HOPG substrates in AuNP solutions in hexane. For BT, concentrations (c) ranging from 0.3 to 2 mg mL^{-1} were used, while for NT c was changed from 0.02 to 2 mg mL^{-1}. Different adsorption times were used (30 min $\leq t_a \leq$ 24 h). After the incubation, the modified substrates were repeatedly rinsed with hexane and dried with nitrogen.

X-ray absorption measurements at the S K-edge and at the Au L_3-edge were performed at the SXS and XAFS1 beamlines of the LNLS respectively (see Supporting Information). X-ray photoelectron spectroscopy (XPS) measurements were performed using a Mg Kα source (XR50, Specs GmbH) and a hemispherical electron energy analyzer (PHOIBOS 100, Specs GmbH). Spectra were acquired with 10 eV pass energy and normalized to the C 1s signal. Scanning tunneling microscopy (STM) imaging was made in air in the constant current mode with a Nanoscope IIIa microscope from Digital Instruments (Santa Barbara, CA) and by using commercial Pt−Ir tips. Typical tunneling currents, bias voltages and scan rates were 30 pA, 1.5 V, and 0.8 Hz, respectively.

Electrochemical measurements were performed in deaerated aqueous 0.1 M NaOH with a Ag/AgCl reference electrode and a high area gold foil as reference and counter electrodes, respectively. All potentials are reported in the Ag/AgCl scale.

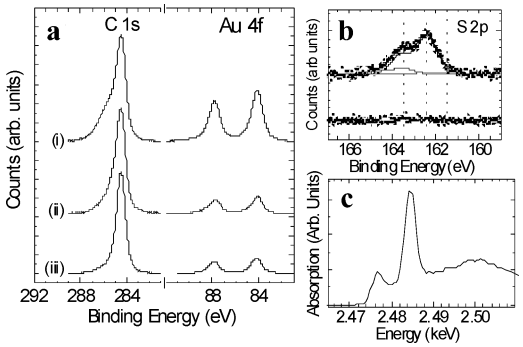

Figure 1. (a) (i) C 1s and Au 4f XPS spectra of butanethiol-capped AuNP on HOPG (c = 2 mg mL^{-1}), (ii) AuNP on HOPG after butanethiol reductive desorption, and (iii) butanethiol-capped AuNP on HOPG (c = 0.3 mg mL^{-1}). (b) S 2p XPS spectra of (up) butanethiol-capped AuNP on HOPG (c = 2 mg mL^{-1}), and (down) AuNP on HOPG after butanethiol reductive desorption. The fit corresponding to the three components is shown. (c) Sulfur XANES K-edge spectrum of butanethiol-capped AuNP supported on HOPG.

Electrodesorption of thiolates from the AuNP supported on HOPG was compared to that measured for thiol-covered smooth and nanostructured rough Au surfaces.[25]

Results and Discussion

Typical XPS spectra of the Au 4f and C 1s regions for AuNP immobilized on HOPG by simple immersion of the substrates in AuNP−containing hexane solutions are shown in Figure 1a (spectra i and iii). The Au/C signal intensity ratio increases with c, indicating that the AuNP surface coverage can be controlled by changing the concentration of the NP (Figure 1a). The XPS S 2p signal at 162 eV (Figure 1b) reveals the presence of Au-thiolate bonds on the gold NP surface.[26] The S/Au signal intensity ratio remains constant irrespective of c, meaning that all AuNP are covered by alkanethiols. No traces of oxidized S, such as sulfonates, were detected, since no signal was observed at 168 eV. The spectrum shown in Figure 1b was fitted by considering the usual three components,[26] corresponding to unbounded thiols (163 eV), chemisorbed thiols (162 eV), and S impurities (161 eV). However, only the contribution of chemisorbed thiols at 162 eV was significant (the 161 and 163 eV components represented only ∼5% and ∼10%, respectively).

The absence of a significant amount of unbounded thiols in the adsorbed NP was confirmed by XANES. To perform this experiment, a few drops of AuNP in hexane solution were put on a carbon tape and then the solvent was evaporated at room temperature. Sulfur K-edge XANES spectra of the AuNP in these conditions consist of a single peak, thus corroborating the presence of free thiols (not bounded to AuNP) in the sample, as already reported.[27] On the other hand, after simply rinsing the adsorbed AuNP on HOPG with hexane, the sulfur K-edge XANES spectra consist of two well-defined peaks (Figure 1c). The first peak (at lower energy) is associated to S−Au, and the second one to the S−C bond from the hydrocarbon chains.[28] Note that no XANES signal was obtained after rinsing with hexane HOPG substrates previously immersed in 0.5 mM thiol solutions. These results indicate that no unbounded thiols are adsorbed on HOPG during thiol-capped AuNP adsorption, although they are indeed present in the original solution. In fact, it has been reported that thiols are weakly physisorbed on HOPG so that they can be easily removed by rinsing with the solvent.[29] In addition, this result shows that there is a selective immobilization of thiol-capped AuNP on the HOPG substrate (i.e., the spectrum arises solely from the thiols in the AuNP surface).

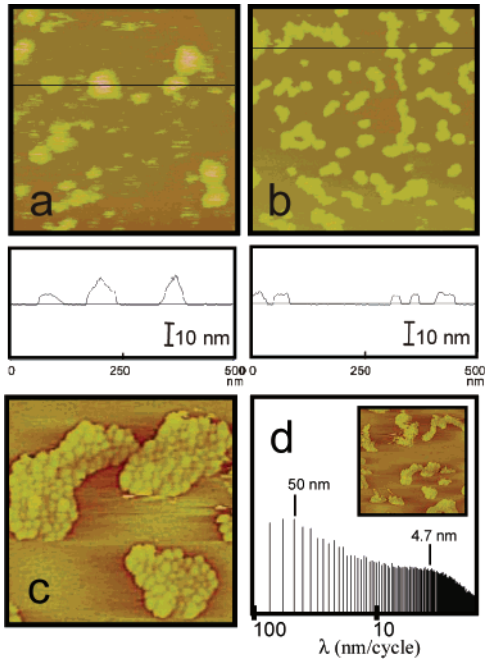

Figure 2. (a, b) 500 × 500 nm^2 STM images of the butanethiol-capped AuNP islands on HOPG in air. (a) 2 mg mL^{-1} solution, t_a = 30 min, and (b) 0.3 mg mL^{-1} solution, t_a = 30 min. The black solid lines in panels a and b indicate the places where the cross-sections were made. (c) 125 × 125 nm^2 STM image of the islands showing that they are formed by individual AuNP. (d) Isotropic 2D power spectral density of the 300 × 300 nm^2 image shown in the inset. The two arrows indicate the average island size and the average particle size.

STM was used to characterize BT-capped AuNP/HOPG surfaces. For the 2 mg mL^{-1} solution and 30 min adsorption time, some regions of the HOPG surface exhibit neither a clear structure, nor any evidence of HOPG steps and terraces. In these regions, the substrate seems to be completely covered by a thin AuNP layer. In other regions, isolated islands 30−50 nm in diameter and 4−18 nm in height were observed on the HOPG terraces (Figure 2a, and cross section). The height of the islands suggests that they involve 1−4 NP layers. Attempts to resolve individual nanoparticles were unsuccessful.

On the other hand, for BT-capped AuNP/HOPG surfaces prepared from the 0.3 mg mL^{-1} solution and 30 min adsorption time, the islands have 4−5 nm in height (Figure 2b). This corresponds to that expected for a BT-capped NP of 3 nm diameter. Inside of the islands, the thiol-capped nanoparticles can be clearly resolved (Figure 2c). The 2D power spectral density made on a 300 nm image of the deposit (Figure 2d, and inset) shows two peaks at 50 and 4.7 nm, corresponding to the average size of the islands and of the individual nanoparticles, respectively.

While AuNP supported on the HOPG surface have been cleaned from adsorbed thiols by thermal desorption by heating the substrate to 300 °C,[20] this procedure could result in NP sintering.[21] We have therefore explored the efficiency of reductive desorption[30] to eliminate the thiols from our AuNP/HOPG system. Some previous results of thiol electrodesorption from AuNP have been already reported, although in that case the thiol had been assembled on the AuNP already immobilized on hydrophilic glassy carbon surfaces.[13] Typical cyclic voltammograms (first scan) for the thiol-capped AuNP supported on HOPG recorded in 0.1 M NaOH between −0.2 V and −1.6 V are shown in Figure 3a.

In the j (current density)/E (potential) profiles it can be seen that, just before the onset of the current associated to the hydrogen evolution reaction (HER), there is an important current peak that can be assigned to the thiol reductive desorption according to the reaction

$$CH_3(CH_2)_{n-1}S{-}Au + e = CH_3(CH_2)_{n-1}S^- + Au \quad (1)$$

Several voltammetric cycles, 2−3 for BT and 4−5 for NT (dashed lines in Figure 3a), are necessary to completely remove traces of thiols from the AuNP/HOPG surface prepared from concentrated NP solutions, i.e., to see the complete elimination of the peak in Figure 3a. This is because small amounts of desorbed thiolates can be readsorbed in the anodic scan on the clean AuNP[31] that remain on the HOPG surface. The XPS spectra after complete butanethiol desorption and careful rinsing of the sample with MilliQ water confirm that the current peak observed in the j/E profile corresponds to thiol desorption. In fact, the S signal at 162 eV has been practically eliminated from the XPS spectrum (Figure 1b, spectrum ii). NT desorbs at potential values more negative than BT due to the stabilizing effect of the hydrocarbon chains (van der Waals interactions) and also due to hydrophobic forces.[30] A plot of the reductive desorption peak potential (E_p) versus n (the number of C atoms in the hydrocarbon chains) for different thiols and gold substrates (smooth gold, nanostructured gold, and AuNP on HOPG) is shown in the inset of Figure 3a. Notably, the E_p values obtained for NT and BT agree very well with those obtained for thiol desorption from nanostructured rough gold electrodes.[32] These values are much more negative than those recorded for smooth Au surfaces, indicating the presence of additional overpotentials for thiol removal from curved and irregular surfaces. Similar results have been observed for dithiol-covered AuNP supported on Au by exchange-cross-linking and assigned to additional barriers for thiolate desorption from edges and corners of the NP.[33] These results of thiol desorption from AuNP could be important to control the potential-induced release of biomolecules and drugs attached to the NP by thiol groups.[34] The slightly smaller slope in the E_p versus n plot with respect to the smooth substrate would reflect the presence of loosely packed hydrocarbon chains, as already suggested.[35]

The presence of the AuNP in the NaOH solution after thiol desorption (in a 1 mL electrochemical cell) has been confirmed by UV−vis spectroscopy measurements. After the thiol desorption from AuNP was performed, the NaOH electrolytic solution was placed in contact with 1 mL of hexane in order to extract the AuNP eventually released during the electrochemical process. The spectrum obtained from this hexane solution is similar to that recorded for the original thiol-capped AuNP in hexane before adsorption on the HOPG surface (Figure 4) Note the absence of the plasmon absorption in the UV−visible spectrum, in accordance with the small size of the AuNP before and after release.[24,36]

Another procedure has been performed to detect the release of AuNP to the NaOH electrolytic solution after thiol desorption. The NaOH solution was put in contact with 1 mL of hexane in order to extract the AuNP released during the electrochemical process. An HOPG substrate was immersed during 24 hs in the hexane extracting solution in order to readsorb the AuNP. The first scan of voltammetric runs corresponding to these HOPG surfaces in 0.1 M NaOH also reveal the typical thiol reductive desorption peaks from the AuNP surfaces shown in Figure 3a. This result confirms not only that the AuNP are released during the reductive desorption but also it suggests that they are again covered by the thiols. Even if we are not able to completely rule out the presence of leftover AuNP from the initial solution, this result is also compatible with the presence of desorbed thiols

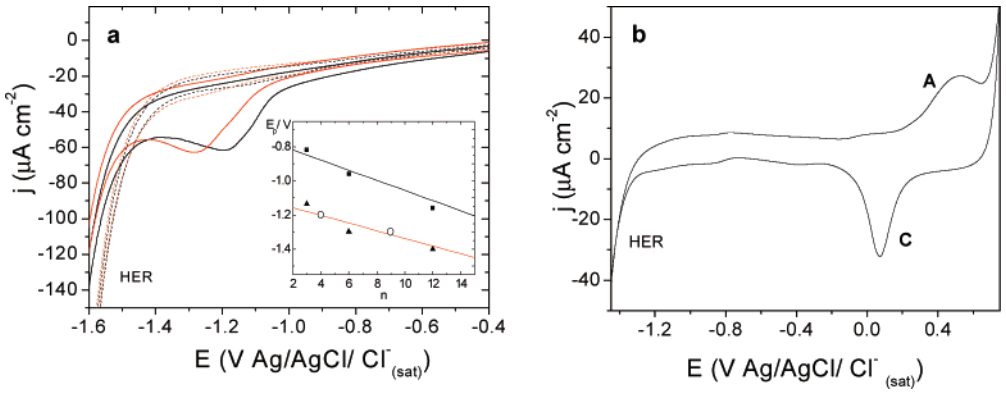

Figure 3. (a) Reductive desorption voltammetric curves (first scan) recorded at 0.05 V s^{-1} in aqueous 0.1 M NaOH for BT-capped (solid line-black) and NT-capped (solid line-red) AuNP on HOPG surfaces. Third scan after BT desorption (dashed line-black) and fifth scan after NT desorption (dashed line-red). Inset: potentials of the reductive peaks (E_p) for NT and BT on AuNP (open circles) are included in E_p vs n plots for thiol-covered smooth Au (filled circles) and nanostructured rough Au (triangles). (b) Typical voltammogram recorded at 0.1 V s^{-1} from 0.7 to −1.4 V in aqueous 0.1 M NaOH for AuNP modified HOPG (solid line) after the complete reductive desorption of thiols. Peaks A and C correspond to the formation and reduction of the AuO monolayer. The current increase starting at −1.25 V is related to the hydrogen evolution reaction (HER).

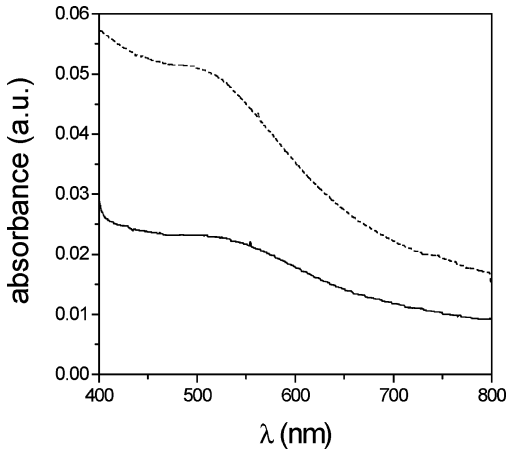

Figure 4. UV visible spectra recorded in hexane for (dashed line) thiol-capped AuNP (0.011 g mL^{-1}) before adsorption on the HOPG surface; (continuous line) after thiol desorption in NaOH and extraction to hexane (0.0066 g mL^{-1}).

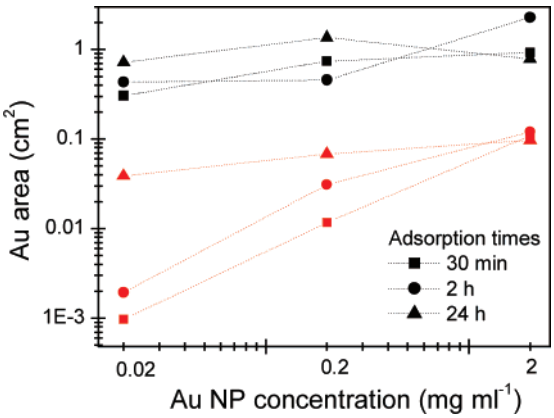

Figure 5. Area of the immobilized AuNP on HOPG, which is proportional to the amount of immobilized nanoparticles. Black: AuNP area estimated from thiol desorption. Red: AuNP area estimated from AuO reduction.

that can again be self-assembled on the clean AuNP in the NaOH solution. In any case, spontaneous adsorption followed by reductive desorption could be a simple route to easily transfer thiol-capped metallic NP from one environment to another.

The electrochemical behavior in 0.1 M NaOH of the thiol-free AuNP that remained adsorbed on HOPG (after several voltammetric cycles, to completely remove thiol molecules) closely resembles that observed for bulk gold electrodes. In fact, the j/E profile in Figure 3b exhibits the typical peaks related to gold oxide electroformation (A) and electroreduction (C) and remains unchanged under repetitive potential scanning between the hydrogen and the oxygen evolution reactions.

In Figure 5 we show the influence of the NP concentration and adsorption time on the Au surface area, a magnitude that is proportional to the amount of electrochemically active nonanethiol-capped AuNP adsorbed on HOPG. The Au surface area before thiol desorption was estimated from the charge density involved in the thiol electrodesorption peaks (Figure 3, see Supporting Information). Figure 5 clearly shows that the amount of AuNP rapidly reaches saturation, being independent of the NP concentration and adsorption time.

In contrast, the surface area derived from the AuO electroreduction peak (Figure 3b), which is proportional to the total amount of AuNP remaining on the HOPG surface after thiol desorption, increases markedly with the NP concentration and is a function of the adsorption time, particularly for the more dilute solutions. Similar results are obtained using the BT-capped AuNP; i.e., there are no marked differences by changing the hydrocarbon chain length.

Results from Figure 5 also show that the total amount of AuNP remaining on the HOPG surface after complete thiol desorption is much smaller (1−10% depending on c) than that estimated before thiol desorption. In Figure 1a it can be seen that the Au 4f/ C 1s XPS peak ratio in spectrum ii is much smaller than that of spectrum i (recorded before reductive desorption), confirming that a significant amount of AuNP has been released to the solution and suggesting that interactions between the thiol capped NP are important to stabilize the system.

The remaining "clean" (thiol-free) AuNP supported on the HOPG do not collapse by sintering. Figure 6 shows the Fourier transform of the EXAFS oscillation and the corresponding fit of the AuNP supported on HOPG (prepared by 20 h immersion in the concentrated solution) after the thiol desorption. The average coordination number for the Au−Au pair obtained from the fit is 9.5 ± 0.9, which is clearly smaller than 12, the corresponding value for the bulk Au material.[27] This result shows that the AuNP retain their identity after reductive thiol desorption and do not sinter. In fact, STM images of this substrate shows uncovered HOPG regions and islands formed by isolated AuNP (Figure 6 inset).

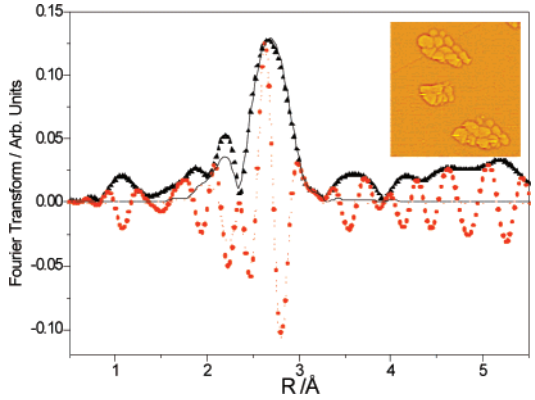

Figure 6. EXAFS data for butanethiol-capped AuNP on HOPG (c = 2 mg mL^{-1}, t_a = 30 min) after thiol desorption. Amplitude (triangles) and imaginary part (circles) of the Fourier transform of the EXAFS signal. Solid lines show the corresponding fitting functions. Inset: 112 × 112 nm^2 STM image in air (highpass treated) of the islands formed by individual AuNP.

Different interactions could be involved in the stabilization of the AuNP on the carbon surfaces. Electrostatic interactions have been proposed between thiol-free citrate stabilized AuNP and hydrophilic glassy carbon surfaces prepared by electrooxidation.[13] Immobilization of small (2−5 nm in size) dithiol-capped AuNP on Au and C has been also reported.[32] In this case the dithiol is introduced by exchange and cross-linking to improve the interaction between AuNP and the substrates. While the importance of the terminal thiol group to interact with the Au surface is obvious, it is not clear if the S−C interaction plays a relevant role in AuNP inmmobilization on carbon. It should be noted, however, that the adsorption of sulfur species on carbon surfaces has been already observed.[37] Our results demonstrate that dithiols are not needed to immobilize the thiol-capped AuNP on hydrophobic carbon surfaces.

In principle, thiol-capped AuNP and HOPG stabilization forces should result from nonpolar hydrocarbon chain-HOPG surface interactions,[38] although a certain contribution of the small amount of sulfur species detected by our XPS data (∼5%) cannot be discarded.[37] However, other contributions should be present, as thiols are easily desorbed from the HOPG surface by simply rinsing with hexane (no S XPS 2p signal can be observed, results not shown), while the AuNP remain there. Photoemission measurements on a femtosecond time scale have revealed partial charge transfer between nanoparticles and HOPG surfaces through alkanethiol monolayers.[39,40] Therefore, it is possible that all these interactions contribute to the stability of the thiol-capped AuNP on the hydrophobic and chemically inert HOPG surface.

Concerning the formation of the AuNP three-dimensional islands, we propose that the adsorbed thiol-capped AuNP on the HOPG surface can trap other nanoparticles arriving from the solution, forming 2D islands. The islands can then grow in 2D, by AuNP incorporation at the island edges, or in 3D, by addition of other NP atop of the islands. This process can explain the shape of the islands observed in the STM images. The interaction between the hydrocarbon chains of the adsorbed thiols also seems to play a role in stabilizing the NP in the islands, as revealed by the large AuNP loss after thiol desorption. In fact, it has been reported that the separation of closely packed AuNP in crystals is linearly dependent on the length of the alkyl chains, although the increase in particle spacing per additional carbon is about one-half of the expected value.[41] This observation suggests that the alkyl chains might interdigitate with the chains on neighboring particles stabilizing the system.

Conclusions

We have demonstrated that carbon surfaces can be modified by simple adsorption of alkanethiol-capped AuNP from hexane solutions. Neither modification of the carbon surface nor introduction of dithiol linkers is needed. The AuNP arrange in layers that are electrically connected to the substrate (a crucial point for applications in electrocatalysis and biosensors) and can be easily cleaned from chemisorbed thiols by simple electroreductive desorption. This procedure could be used to directly modify carbon nanotubes or to metallize carbon surfaces using an extremely low amount of material. It is then possible to prepare gold-like substrates with a very small amount of high-quality AuNP without using electrodeposition or physical vapor deposition (which requires more sophisticated equipment and implies a lesser control on size distribution of NP). This could be extended to graphite powder or activated carbon, and also to nonconductive solids. Finally, high-area carbon surfaces can be used to remove metallic NP from solutions (useful for decontamination purposes), or from biological systems (important in relation to AuNP toxicity).

Moreover, the reductive desorption of thiols from the carbon surface produces an efficient release of the AuNP from carbon surfaces to the aqueous solution. Therefore, this procedure can be used to transfer thiol-capped NP from one environment to another. Our results also envisage that thiol reductive desorption from thiol-capped AuNP supported on biocompatible carbon surfaces (i.e., carbon nanotubes)[42] can be an efficient method to release the NP carrying drugs or biomolecules into living cells by simply applying a small electric voltage or current.

Acknowledgment. This work was supported by the Agencia Nacional de Promoción Científica y Tecnológica (PICT 02-11111 and 06-17492), CONICET (PIP 0675 and CIAM Collaborative Project), Universidad Nacional de La Plata (Argentina), and Laboratorio Nacional de Luz Sincrotron (LNLS, Campinas, Brazil) (under projects D04B-XAS # 3492/04, D11A-SAXS # 2832/04, and D04A-SXS # 2311/03). This paper was made in the frame of the Argentine Nanotechnology Networks.

Supporting Information Available: The method for AuNP preparation, AuNP size distribution (SAXS measurements), XANES and UV characterization, and the estimation of the amount of deposited AuNP by electrochemical methods are presented in the Supporting Information. The methods for the preparation of smooth and rough gold substrates are also included. This material is available free of charge via the Internet at http://pubs.acs.org.

References and Notes

(1) Bell, A. T. *Science* **2003**, *299*, 1688, Fu, Q.; Saltsburg, H.; Flytzani-Stephanopoulos, M. *Science* **2003** *301*, 935, Hutchings, G. J.; Haruta, M. *Appl. Catal., A* **2005**, *291*, 2.

(2) Sivakumar, P.; Ishak, R.; Tricoli, V. *Electrochim. Acta* **2005**, *50*, 3312.

(3) Xian, Y.; Hu, Y.; Liu, F.; Xian, Y.; Wang, H.; Jin, L. *Biosens. Bioelectron.* **2005** *21*, 1996. Yang, K.; Wang, H.; Zou, K.; Zhang, X. *Nanotechnology* **2006** *17*, S276−S279. Glynou, K; Ioannou, P. C.; Christopoulos, T. K.; Syriopoulou, V. *Anal. Chem.* **2003**, *75*, 4155.

(4) Baker, G. A.; Moore, D. S. *Anal. Bioanal. Chem.* **2005**, *382*, 1751.

(5) Zhang, P.; Zhou, X. T.; Tang, Y. H.; Sham, T. K. *Langmuir* **2005**, *21*, 8502. Zhu, J.; Kenya, Z.; Puntes, V. F.; Kiricsi, I.; Miao, C. X.; Ager, Z. W.; Alivisatos, P.; Somorjai, G. A. *Langmuir* **2003**, *19*, 4396.

(6) Takele, H.; Schürmann, U.; Greve, H.; Paretkar, D.; Zaporojtchenko, V.; Faupel, F. *Eur. Phys. J. Appl. Phys.* **2006**, *33*, 83.

(7) Yamanoi, Y.; Sirahata, N.; Yonezawa, T.; Terasaki, N.; Yamamoto, N.; Matsui, Y.; Nishio, K.; Masuda, H.; Ikuhara, Y.; Nishihara, H. *Chem. Eur. J.* **2006**, *12*, 314.

(8) El-Deab, M. S.; Ohsaka, T. *J. Electrochem. Soc.* **2006**, *153*, A1365.

(9) Brust, M.; Kiely, C. J.; *Colloids Surf. A* **2002**, *202*, 175.

(10) Daniel, M. C.; Astruc, D. **2004** *Chem. Rev. 104*, 293.

(11) Gittins, D. I.; Bethell, D.; Schiffrin, D. J.; Nichols, R. J. *Nature* **2000** *408*, 67. Rawlett, A. M.; Hopson, T. J.; Amlani, J.; Zhang, R.; Tresek, J.; Nagahara, L. A.; Tsui, R. A.; Goronkin, H. *Nanotechnology* **2000**, *14*, 377. Kiely, C. J.; Finck, J.; Brust, M.; Bethell, D.; Schiffrin, D. J.; *Nature* **1998**, *396*, 444.

(12) Rosi, N. L.; Giljohann, D. A.; Thaxton, C. S.; Lytton-Jean, A. K. R.; Han, M. S.; Mirkin, C. A. *Science* **2006**, *312*, 1027.

(13) Shin, H.; Kang, C. *Anal. Sci.* **2003**, *19*, 1667.

(14) Carrillo, A.; Swartz, J. A.; Gamba, J. M.; Nirupama Chakrapani, R. S. K.; Wei, B.; Ajayan, P. M. *Nano Lett.* **2003**, *3*, 1437.

(15) Zhang, L.; Zhang, J.; Schmandt, N.; Cratty, J.; Khabashesku, V. N.; Kelly, K. F.; Barron, A. R. *Chem. Commun.* **2005**, *43*, 5429.

(16) Ou, Y-Y.; Huang, M. H. *J. Phys. Chem. B* **2006**, *110*, 2031.

(17) Kim, K.; Lee, S. H.; Yi, W.; Kim, J.; Choi, J. W.; Park, Y.; Jin, J-I *Adv. Mat.* **2003**, *15*, 1618.

(18) Ellis, A. V.; Vijayamohanan, K.; Goswami, R.; Chakrapani, N.; Ramanathan, L.; Ajayan, P. M.; Ramanath, G. *Nano Lett.* **2003**, *3*, 279.

(19) Correa-Duarte, M. A.; Liz-Marzan, L. M. *J. Mater. Chem.* **2006**, *16*, 22.

(20) Tominaga, M.; Shimazoe, T.; Nagashima, M.; Kusuda, H.; Kubo, A.; Kuwahara, Y.; Taniguchi, I. *J. Electroanal. Chem.* **2006**, *590*, 37.

(21) Fullam, S.; Cottell, D.; Rensmo, H.; Fitzmaurice, D. *Adv. Mater.* **2000**, *12*, 1430. Martin, J. E.; Odinek, J. T.; Wilcoxon, J. P.; Anderson, R. A.; Provencio, P. *J. Phys. Chem. B* **2003**, *107*, 430. Shimizu, T.; Teranishi, T.; Hasegawa, S.; Miyake, M. *J. Phys. Chem. B* **2003**, *107*, 2719.

(22) Kim, S. H.; Hwang, S.; Shon, Y-S.; Ogletree, D. F.; Salmeron, M. *Phys. Rev. B* **2006**, *73*, 155406.

(23) Santini, J. T., Jr.; Cima, M. J.; Langer, R. *Nature* **1999**, *397*, 335. Paciotti, G. F.; Myer, L.; Weinreich, D.; Goia, D.; Pavel, N.; McLaughlin, R. E.; Tamarkin, L.; *Drug Delivery* **2004**, *11*, 169. Emerich, D. F.; Thanos, C. G. *Biomol. Eng.* **2006**, *23*, 171. Kogan, M. J.; Bastus, N. J.; Amigo, R.; Grillo-Bosch, D.; Araya, E.; Turiel, A.; Labarta, A.; Giralt, E.; Puntes, V. F. *Nano Lett.* **2006**, *6*, 110.

(24) Brust, M.; Walker, M.; Bethell, D.; Schiffrin, D. J.; Whyman, R. *Chem. Commun.* **1994**, *40*, 801.

(25) Salvarezza, R. C.; Arvia, A. J. In *Modern Aspects of Electrochemistry*; Conway, B. E., Bockris J. O'M., White R. E., Eds.; Plenum Press: New York, 1996; Vol. 28, Chapter 5, pp 289−373.

(26) Zhong, C. J.; Brush, R. C.; Anderegg, J.; Porter, M. D. *Langmuir* **1999**, *15*, 518.

(27) Ramallo-López, J. M.; Giovanetti, L. J.; Requejo, F. G.; Isaacs, S. R.; Shon, Y. S.; Salmeron, M. *Phys. Rev. B* **2006**, *74*, 073410.

(28) Zhang, P.; Sham, T. K. *Appl. Phys. Lett.* **2003**, *82*, 1778.

(29) Terán Arce, F.; Vela, M. E.; Salvarezza, R. C.; Arvia, A. J. *Surf. Rev. Lett.* **1997**, *4*, 637.

(30) Vela, M. E.; Martin, H.; Vericat, C.; Andreasen, G.; Hernández Creus, A.; Salvarezza, R. C. *J. Phys. Chem. B* **2000**, *104*, 11878.

(31) Yang, D. F.; Wilde, C. P.; Morin, M. *Langmuir* **1996**, *12*, 6570; Yang, D. F.; Al-Maznai, H.; Morin, M. *J. Phys. Chem. B* **1997**, *101*, 1158.

(32) Vericat, C.; Benitez, G-A.; Vela, M. E.; Salvarezza, R. C.; Tognalli, N-G.; Fainstein, A. *Langmuir* **2007**, *23*, 1152.

(33) Leibowitz, F. L.; Zheng, W.; Maye, M. M.; Zhong, C.- *J. Anal. Chem.* **1999;** *71*, 5076. Zhong, C J; Zheng, W. X.; Leibowitz, F. L. *Electrochem. Commun.* **1999**, *1*, 72.

(34) Rena, L.; Chowa, G. M. *Mater. Sci. Eng., C* **2003**, *23*, 113; Wiedera, M. E.; Honea, D. C.; Cooka, M. J.; Handsleyb, M. M.; Gavrilovicb, J.; Russell, D. A. *Photochem. Photobiol. Sci.* **2006**, *5*, 727.

(35) Templeton, A. C.; Hostetler, M. J.; Kraft, C. T.; Murray, R. W. *J. Am. Chem. Soc.* **1998**, *120*, 1906.

(36) Zhang, P.; Sham, T. K. *Phys. Rev. Lett.* **2003**, *90*, 245502.

(37) Zubimendi, J. L.; Salvarezza, R. C.; Vázquez, L.; Arvia, A. J. *Langmuir* **1996**, *12*, 2.

(38) Lux, F.; Lemercier, G.; Andraud, C.; Schull, G.; Charra, F. *Langmuir* **2006**, *22*, 10874.

(39) Tanaka, A.; Takeda, Y.; Nagasawa, T.; Sato, S. *Phys. Rev. B* **2003**, *67*, 033101.

(40) Lopez-Salido, I.; Lim, D. C.; Dietsche, R.; Bertram, N.; Kim, Y. D. *J. Phys. Chem. B* **2006**, *110*, 1128.

(41) Martin, J. E.; Wilcoxon, J. P.; Odinek, J.; Provencio, P. *J. Phys. Chem. B* **2000**, *104*, 9475. Wang, Z. L.; Harfenist, S. A.; Vezmar, I.; Whetten, R. L.; Bentley, J.; Evans, N. D.; Alexander, K. B. *Adv. Mater.* **1998**, *10*, 808.

(42) Magrez, A.; Kasas, S.; Salicio, V.; Pasquier, N.; Seo, J. W.; Celio, M.; Catsicas, S.; Schwaller, B.; Forró, L. *Nano Lett.* **2006**, *6*, 1121.